Supplementary Material

A) Authors

Name	Location	Contribution
Annelise Y. Mah-Som, MD, PhD	Washington University in St. Louis, St. Louis	Reviewed and interpreted patient data, drafted the manuscript
Cristina Skrypnyk, MD, PhD	Arabian Gulf University, Bahrain	Collected patient data, revised the manuscript for intellectual content
Andrea Guerin, MD	Queen's University Kingston	Collected patient data, revised the manuscript for intellectual content
Raafat Hammad Seroor Jadah, MBBCh, AB Ped, SB Ped	Bahrain Defense Forces Royal Medical Services Hospital, Bahrain	Collected patient data, revised the manuscript for intellectual content
Vinayak Nivrutti Vardhan, MBBS, DCH	Bahrain Defense Forces Royal Medical Services Hospital, Bahrain	Collected patient data, revised the manuscript for intellectual content
Robert C. McKinstry, MD PhD	Washington University in St. Louis, St. Louis	Reviewed patient imaging, revised the manuscript for intellectual content
Marwan S. Shinawi, MD	Washington University in St. Louis, St. Louis	Conceptualized and coordinated study, revised the manuscript for intellectual content

B) Methods

Genetic analysis

DNA was isolated from the probands and their parent's blood samples or cheek swabs using standard methods.

Analysis from GeneDx used their usual protocol: an Illumina system was used to obtain sequences which were then aligned to human genome build GRCh37/UCSC hg19 and analyzed using Xome Analyzer. Pathogenic variants were confirmed by capillary

sequencing or other appropriate method, and variants in the proband were compared to parental samples.

For Patient 5, exome enrichment was performed using Agilent SureSelectVT Human All Exon 5Mb with subsequent sequencing on the Illumina HiSeq platform. Reads were aligned using the Burrows-Wheeler Aligner software, with variant calling using GATK by BGI Europe Denmark. Targeted analysis for intellectual disabilities was done using gene panel version DG-2.5; variant annotation, selection and prioritizing was done by Genome Diagnostics Nijmegen at Radboud University.

For Patient 6, exome analysis was done by Mendelics using an Illumina platform, with alignment to human genome build GRCh37.

C) Figures

Figure e-1. Facial features, ichthyosis, and keratoderma in CEDNIK patients. A-B)
Patient 1 (age 18) and **C-D**) Patient 2 (age 12) display mild hypotelorism and
keratoderma of the soles of the feet. **E**) Patient 3 (age 8) displays microcephaly,
bitemporal narrowing, thick eyebrows, epicanthal folds, flared nares with a bulbous
nasal tip, and F) dry skin over her eyelids and chin. **G**) Patient 4 (age 3) displays
plagiocephaly, thin hair at the temporal region, strabismus, and **H**) ichthyosis near her
G-tube site. **I**) Patient 5 (age 6) displays short forehead with bitemporal narrowing, low-
set ears, microphthalmia, high-arched palate. epicanthal folds, strabismus, anteverted
nares, a short philtrum with bowed upper lip, micrognathia, a high-arched palate, and **J**)
generalized ichthyosis, here shown on the back. Patient 6 (age 2) displays **K**)
synophrys, hirsutism of the forehead, bushy eyebrows, epicanthal folds, a broad,
depressed nasal bridge, and **L**) typical plantar keratoderma.
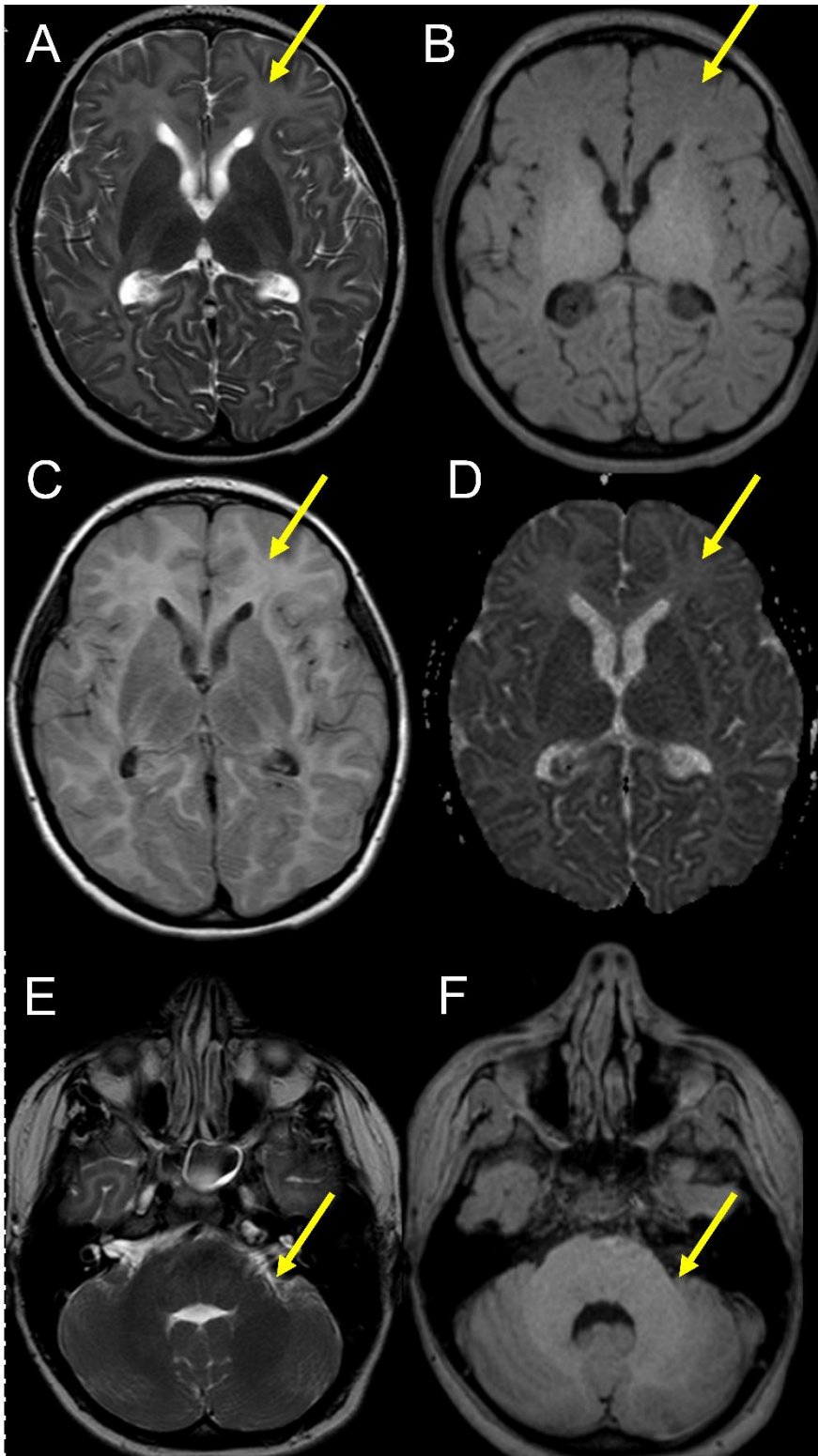
Figure e-2: MR imaging of Patient 1 at 12 years old. A) T2W axial of cerebrum, **B**) T1W axial of cerebrum, **C**) T2W-FLAIR axial of cerebrum, **D**) ADC axial of cerebrum, **E**) T2W axial of cerebellum, **F**) T1W axial of cerebellum. These images show an abnormal myelination pattern for age. **A-D** demonstrate a complete lack of myelinated supratentorial white matter. The yellow arrows point to unmyelinated white matter in the left frontal lobe. **E-F** demonstrate preserved white matter myelination in the posterior fossa. The yellow arrows point to normally myelinated white matter in the left middle cerebellar peduncle.
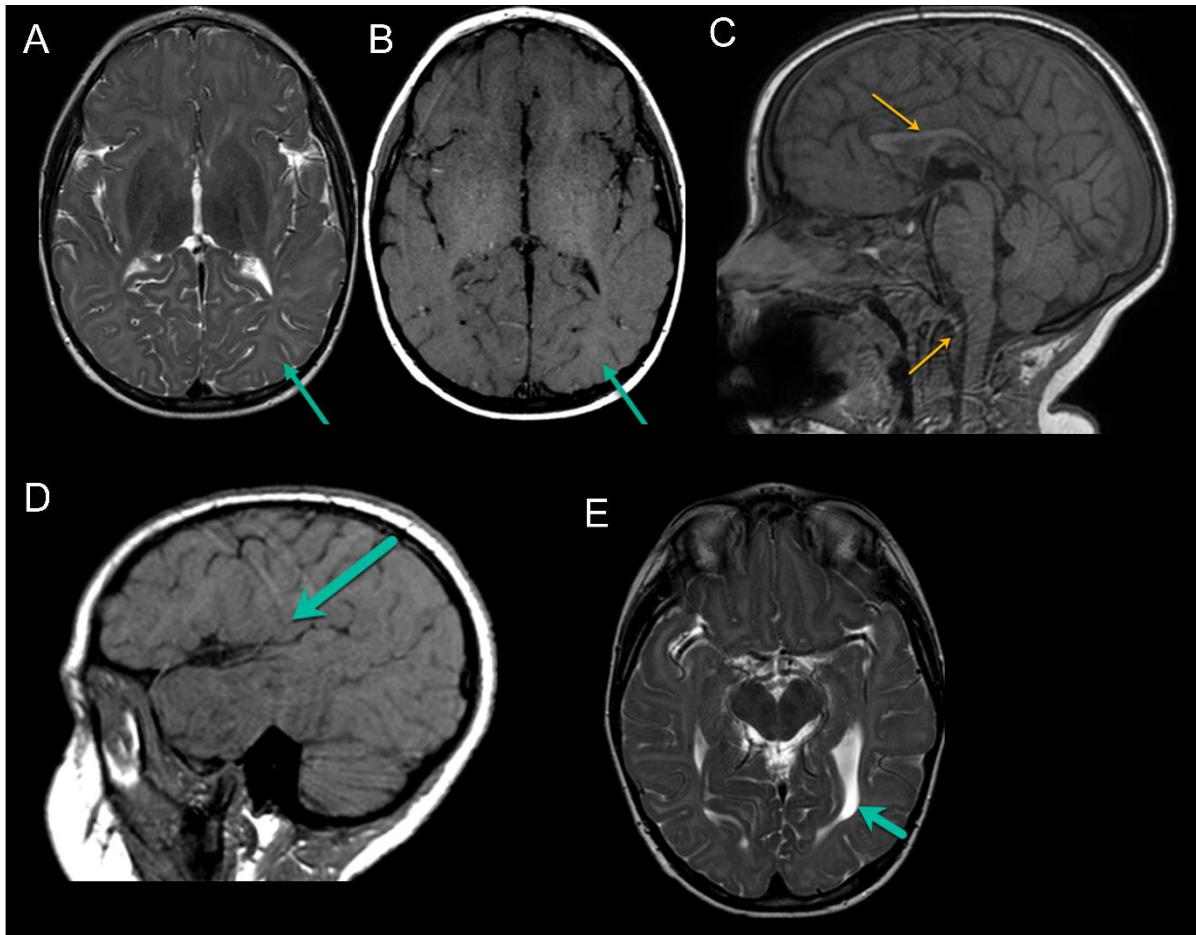
Figure e-3: MR imaging of Patient 2 at 8 years old. A) T2W axial, **B**) T1W axial. These images demonstrate a complete lack of myelinated supratentorial white matter, a similar abnormal myelination pattern as Patient 1. The cyan arrows point to unmyelinated white matter in the left occipital lobe. **C**) T1W sagittal illustrating dysgenesis of the corpus callosum and an abnormal craniocervical configuration and narrowing of the foramen magnum (orange arrows), similar to Patient 1. **D**) T1W sagittal image illustrating an elongated, slightly open Sylvian fissure. **E**) T2W axial image showing thinning of the occipital white matter with associated prominence to the occipital horn of the left lateral ventricle.
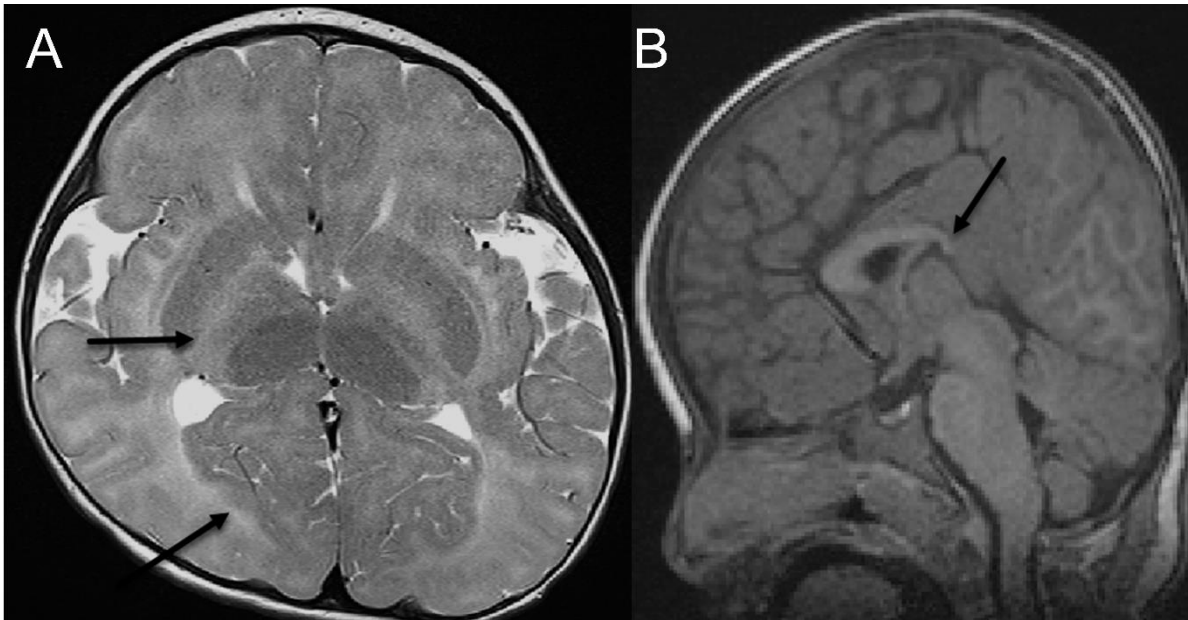
Figure e-4. MR images from Patient 4 at 2 years old. A) T2W axial image illustrating absent myelination signal in the supratentorial white matter. The black arrows point to the posterior limb of the internal capsule and optic radiations, two structures typically hypointense on T2W image by 6 months of age. Other findings on this image include small frontal lobes, open, elongated Sylvian fissures, T2 hyperintensity of the globus pallidus bilaterally, and plagiocephaly of the right occipital region. **B**) T1W sagittal image showing callosal dysgenesis with a deficient splenium (black arrow). The craniocervical junction is also abnormal with narrowing at the foramen magnum and subtle kinking of the medulla oblongata.
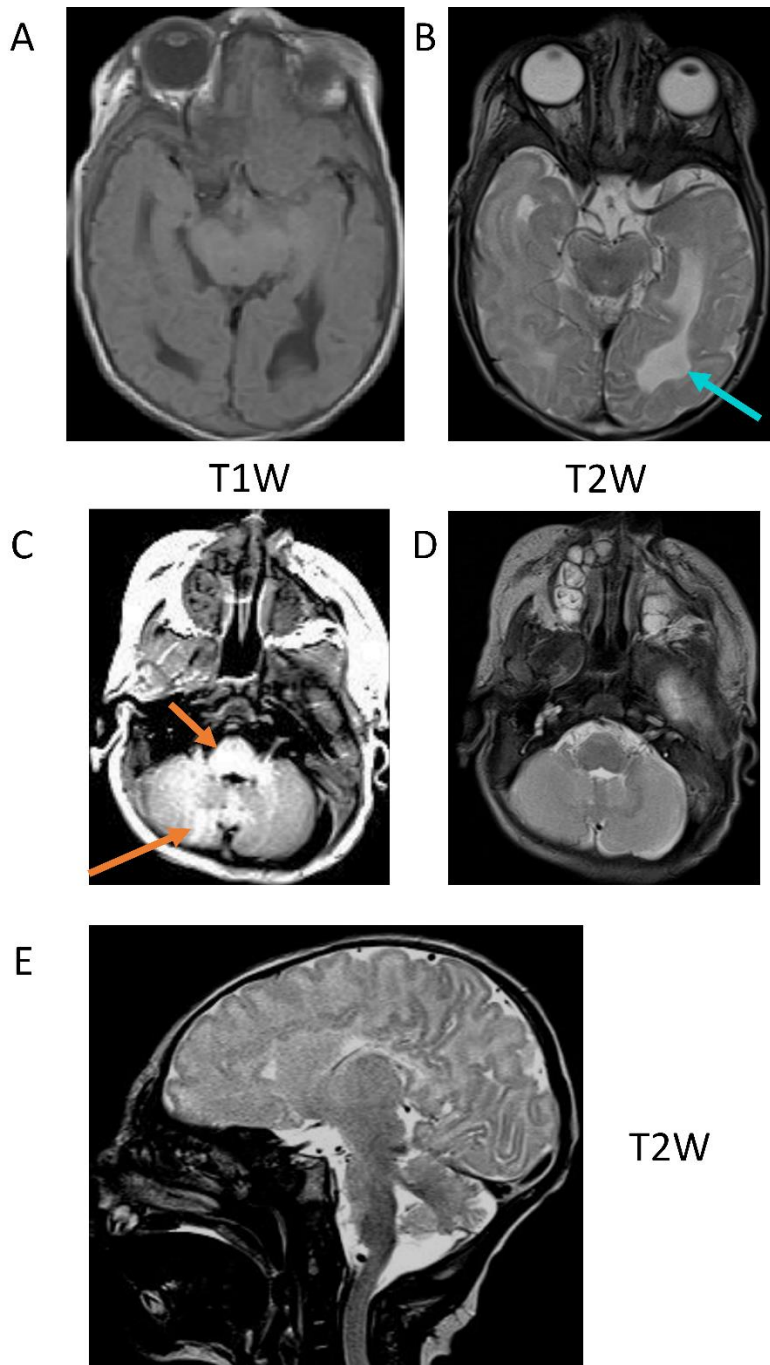
Figure e-5. MR images from Patient 5 at 4 days old. A) T1-weighted axial and **B**) T2-weighted axial images of the cerebrum show prominence of the occipital horns of the lateral ventricles (cyan arrow). At birth, myelination has occurred in select places including the cerebellum and brainstem but is mostly absent in the cerebrum. In this infant, **C**) T1 and **D**) T2 imaging show normal myelination pattern in the posterior fossa (orange arrows). **E**) This T2W sagittal image illustrates small frontal lobes and an abnormal craniocervical junction with narrowing of the foramen magnum; callosal dysgenesis is also present but better seen on T1-weighted sequences.